

Physics beyond the Standard Model with the NA62 experiment at CERN

Letizia Peruzzo^{1,*}

Johannes Gutenberg Universität Mainz Institut für Physik and PRISMA⁺ Cluster of Excellence, Staudingerweg 7, Mainz 55128, Germany.

E-mail: letizia.peruzzo@cern.ch

The NA62 experiment at CERN took data in 2016-2018 with the main goal of measuring the $K^+ \rightarrow \pi^+ \nu \bar{\nu}$ decay. The high-intensity setup and detector performance make NA62 particularly suited for searching for new-physics effects from different scenarios involving feebly-interacting particles in the MeV-GeV mass range. A wide spectrum of exotic K^+ decays were investigated, resulting in stringent upper limits ($O(10^{-10} - 10^{-11})$) on the rate of several lepton number and lepton flavor violating processes. Additionally, searches for $K^+ \rightarrow \ell^+ N$ were performed, where N is assumed to be a heavy neutral lepton decaying to an invisible final state. The results are expressed as upper limits of $O(10^{-8})$ of the neutrino mixing parameter $|U_{\ell 4}|^2$. NA62 can also be run as a beam-dump experiment, when the kaon production target is removed and the upstream collimators are moved into a closed position. Analysis of the data collected in beam-dump mode were performed to search for visible decays of exotic mediators, with particular emphasis on dark-photon models.

*8th Symposium on Prospects in the Physics of Discrete Symmetries (DISCRETE 2022)
7-11 November, 2022
Baden-Baden, Germany*

*Speaker

¹On behalf of the NA62 Collaboration.

1. The NA62 experiment

The NA62 experiment is the latest in a series of fixed-target experiments located at the CERN SPS using the decay-in-flight technique to explore kaon decays. The experiment aims to precisely measure the branching ratio of the very rare decay $K^+ \rightarrow \pi^+ \nu \bar{\nu}$ with at least 20% accuracy, collecting up to 100 events in a few years of data taking. About 4×10^{12} kaon decays were collected during the data-taking period 2016-2018 (referred to as NA62 Run1) and the result of the corresponding branching ratio (BR) measurement is $\text{BR}(K^+ \rightarrow \pi^+ \nu \bar{\nu}) = (10.6 \pm 4.0) \times 10^{-11}$ [1]. Moreover, NA62 serves as a multi-purpose experiment covering a broad kaon and beam-dump physics program.

A detailed description of the experiment can be found in [2]. NA62 uses the SPS 400 GeV/c proton beam, which hits on a beryllium target and produces a secondary hadron beam, with kaons contributing to 6% of all particles. The beam has a momentum of (75 ± 1) GeV/c and a nominal intensity of 750 MHz. The beryllium target is followed by two 1.6 m long, water-cooled, copper collimators (TAX) consisting on a series of graduated holes in which the beam passes through, while the non interacting primary protons and unwanted secondary particles are absorbed. Together with the standard data-taking mode, the experiment can operate in a beam-dump configuration to search for new-physics particles too heavy to be produced directly in kaon decays. In the beam-dump mode, the beryllium target is lifted from the beam line and the TAX collimators are closed, dumping the 400 GeV/c proton beam directly on the TAX. The attenuation provided by the dump allows operating the proton beam well above the nominal intensity of the standard kaon operation.

The detector apparatus (Figure 1) extends over 270 m from the target to the end of the experiment. Tagging and a precise timing of the beam kaons are provided by a Cherenkov detector

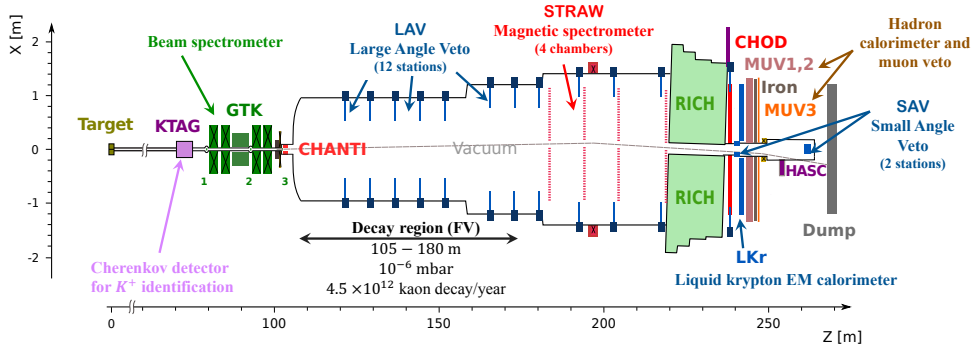


Figure 1: Schematic layout of the NA62 experiment in the X-Z plane.

(KTAG), followed by three silicon pixel stations which form the beam spectrometer (Gigatracker or GTK). A magnetic spectrometer made of four STRAW chambers placed in vacuum provides the momenta and directions of the charged particles reaching the decay volume. The particle identification is performed by a Ring Imaging Cherenkov (RICH) detector, an electromagnetic (LKr) calorimeter, a hadron calorimeter (counting of two modules MUV1 and MUV2) and a muon counter (MUV3). A Large Angle (LAV) and a Small Angle (SAV) Veto form together with the LKr calorimeter the high-efficiency photon-veto system, covering angles from 0 to 50 mrad. A pair of charged hodoscopes (CHOD) provide the timing for the tracks of the final state particles.

The experimental setup is completed by a scintillator detector (CHANTI) and a hadron calorimeter (HASC) to reduce critical background induced by inelastic interactions of the beam with the final collimator and the GTK, and background from kaon decays with particle products traveling along the beam line. The overall time resolution of the experiment reaches $O(100)$ ps and the detectors have to stand a rate of about 10 MHz of events. For these purposes high-performance read-out and trigger systems have been developed [3, 4].

2. Lepton number and lepton flavor violating decays

This section reports the results on the search for lepton number and lepton flavor violating K^+ decays obtained by the analysis of the world's largest data set of charged kaon decays to di-lepton final states collected by NA62 in 2016-2018. Lepton number (LN) and lepton flavor (LF) are conserved numbers in the Standard Model (SM), although their conservation is not imposed by any local gauge symmetry. Neutrino oscillation provided the first hint of the LF non-conservation, which implies an extension of the SM, however so far no evidence of LN violation has been observed. The observation of LN or LF violation would be, therefore, a clear indication of new physics. Many extension of the SM, aiming to explain neutrino properties, predict LN and LF violation in charged processes. A heavy Majorana neutrino could mediate the $K^+ \rightarrow \pi^- \ell^+ \ell^+$ process [5], while the decay $K^+ \rightarrow \pi^+ \ell_1^+ \ell_2^-$ with two leptons of different flavor could be mediated by a leptoquark [6]. Therefore, the observation of such types of interaction would not only reveal more about neutrinos but it could give more insight into other properties of the SM.

Table 1 summarizes the results obtained by NA62 on LN and LF violating decays. Channels with different final states are investigated by blind analyses principle. Although no signs of LN or LF violation are observed, these results set the current world's most stringent upper limits (UL) on the branching ratios, improving considerably over the previous best results. Of particular

Decay channel	Previous BR UL [8]	NA62 BR UL	Improvement
$K^+ \rightarrow \pi^- \mu^+ \mu^+$	8.6×10^{-11}	4.2×10^{-11} [9]	\sim factor 2
$K^+ \rightarrow \pi^- e^+ e^+$	6.4×10^{-10}	5.3×10^{-11} [10]	\sim factor 12
$K^+ \rightarrow \pi^- \pi^0 e^+ e^+$	–	8.5×10^{-11} [10]	first search
$K^+ \rightarrow \pi^- \mu^+ e^+$	5.0×10^{-10}	4.2×10^{-11} [11]	\sim factor 12
$K^+ \rightarrow \pi^+ \mu^- e^+$	5.2×10^{-10}	6.6×10^{-11} [11]	\sim factor 8
$\pi^0 \rightarrow \mu^- e^+$	3.4×10^{-9}	3.2×10^{-10} [11]	\sim factor 10
$K^+ \rightarrow \mu^- \nu e^+ e^+$	2.1×10^{-8}	8.1×10^{-11} [12]	\sim factor 250

Table 1: Summary table on the search for LN and LF violating K^+ decays with NA62 Run1 data.

interest is the channel $K^+ \rightarrow \mu^- \nu e^+ e^+$ ($K_{\mu\nu ee}$), which can violate LN or LF depending on the flavor of the neutrino in the final state. The only previous search for this process dates back to the Geneva-Saclay experiment in 1976 [7]. The SM $K^+ \rightarrow \pi^+ e^+ e^-$ decay is used for the normalization. The signal region is defined in terms of the reconstructed invariant mass in the range 470-505 MeV/ c^2 for the normalization sample and, in terms of the square of the missing invariant mass $m_{\text{miss}}^2 = (P_K - P_\mu - P_e - P_e)^2$ (where P_i is the reconstructed 4-momentum of the i particle)

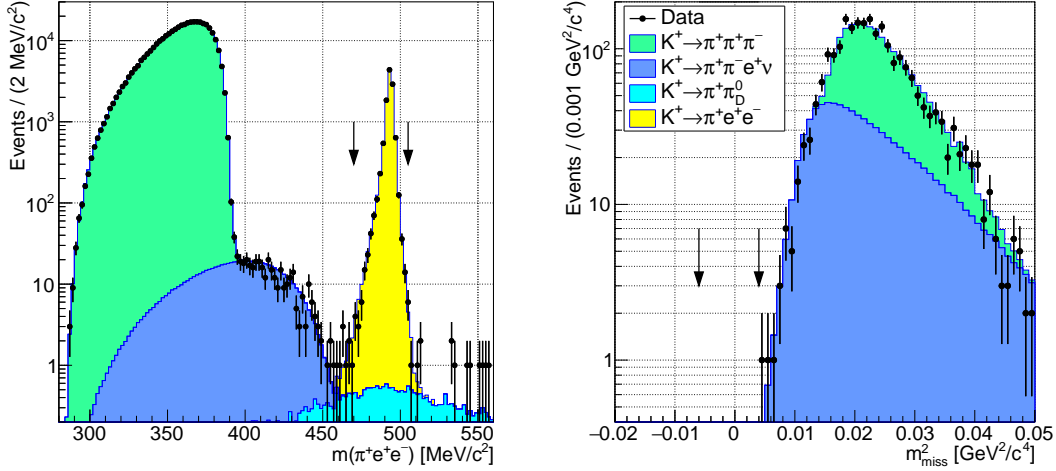


Figure 2: **Left:** Reconstructed $m_{\pi ee}$ invariant mass for data and simulated samples obtained after the $K^+ \rightarrow \pi^+ e^+ e^-$ selection, used as normalization. **Right:** Reconstructed squared missing mass m_{miss}^2 (as defined in the text) spectra after the $K_{\mu\text{vee}}$ selection, data overlaid with simulated background estimates. The normalization and signal mass regions are indicated by vertical arrows. Figure from [12].

for the signal channel in the region $-0.006 \text{ GeV}^2/c^4 < m_{\text{miss}}^2 < 0.004 \text{ GeV}^2/c^4$. Events selected for the normalization and signal samples are shown in Figure 2. The number of expected background events in the signal region of the LN/LF violating decay is $N_{\text{bkg}}^{\text{exp}} = 0.26 \pm 0.04$, originating from $K^+ \rightarrow \pi^+ \pi^- e^+ \nu$ events with the π^+ mis-identified as a positron and the $\pi^- \rightarrow \mu^- \nu$ decaying in flight. No events are observed in the $K_{\mu\text{vee}}$ signal region, resulting in an upper limit on the branching ratio of $\text{BR}(K_{\mu\text{vee}}) < 8.1 \times 10^{-11}$ at 90% confidence level (CL).

3. Search for heavy neutral leptons

This section reports a search for heavy neutral lepton (HNL) production in $K^+ \rightarrow \ell^+ N$ decays (where N denotes the HNL) performed at NA62 with Run1 data in two independent analyses, with a positron [13] or a muon [14] in the final state. In both cases the HNL is supposed to escape detection as long lived. HNLs are hypothesized in many extensions of the SM to generate, via the seesaw mechanism, non-zero masses of the SM neutrinos. In the Neutrino Minimal Standard Model [15] neutrino masses, dark matter, and baryogenesis are accounted for by the introduction of two HNLs in the MeV-GeV mass range and of a third HNL, a dark matter candidate, at the keV mass scale. HNL production in meson decays arises from the mixing between sterile and active neutrinos. In kaon decays the expected branching ratio of $K^+ \rightarrow \ell^+ N$ is [16]

$$\text{BR}(K^+ \rightarrow \ell^+ N) = \text{BR}(K^+ \rightarrow \ell^+ \nu) \cdot \rho_{\ell}(m_N) \cdot |U_{\ell 4}|^2 \quad (1)$$

where $\text{BR}(K^+ \rightarrow \ell^+ \nu)$ is the branching ratio of the SM leptonic decay, $\rho_{\ell}(m_N)$ is a kinematic factor which depends on the HNL mass m_N , and $|U_{\ell 4}|^2$ is the mixing parameter between the SM neutrino and the HNL. The strategy of these analysis is to search for a spike in the missing mass spectrum $m_{\text{miss}}^2 = (P_K - P_{\ell})^2$, where P_i are the reconstructed 4-momenta of the particles, that would correspond to the HNL mass m_N . Figure 3 shows the missing mass distribution for the

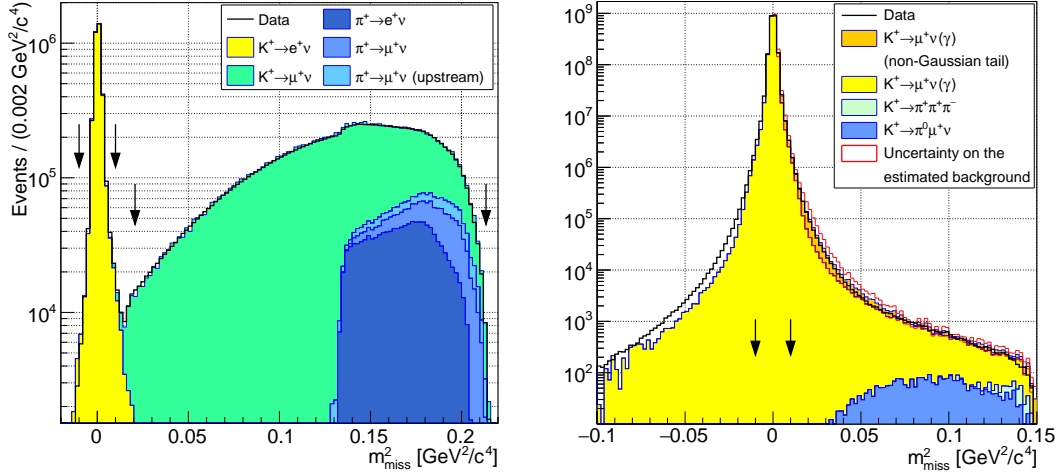


Figure 3: Left: Reconstructed squared missing mass distributions for data and simulated events in the final sample. Decays to muons contribute via muon decays in flight. The boundaries of the SM signal region (upper rows) and the HNL search region (lower rows) are indicated. Figure from [13]. **Right:** Reconstructed m_{miss}^2 distributions for data and the estimated background. The full uncertainties ($\pm 1\sigma$) in each mass bin of the background spectrum for $m_{\text{miss}}^2 > 0$ are shown with a contour. The boundaries of the SM signal region $|m_{\text{miss}}^2| < 0.01 \text{ GeV}^2/c^4$, used for normalization, are indicated with arrows. Figure from [14].

selected events in the positron (left panel) and muon (right panel) signal samples. The scan in m_N is performed in steps of $O(1) \text{ MeV}/c^2$ in mass range $114\text{--}462 \text{ MeV}/c^2$ and $200\text{--}384 \text{ MeV}/c^2$ for the positron and muon channel, respectively. The resulting upper limits on $|U_{e4}|^2$ and $|U_{\mu 4}|^2$ are plotted in Figure 4 together with results from previous searches. In the muon channel, the analysis

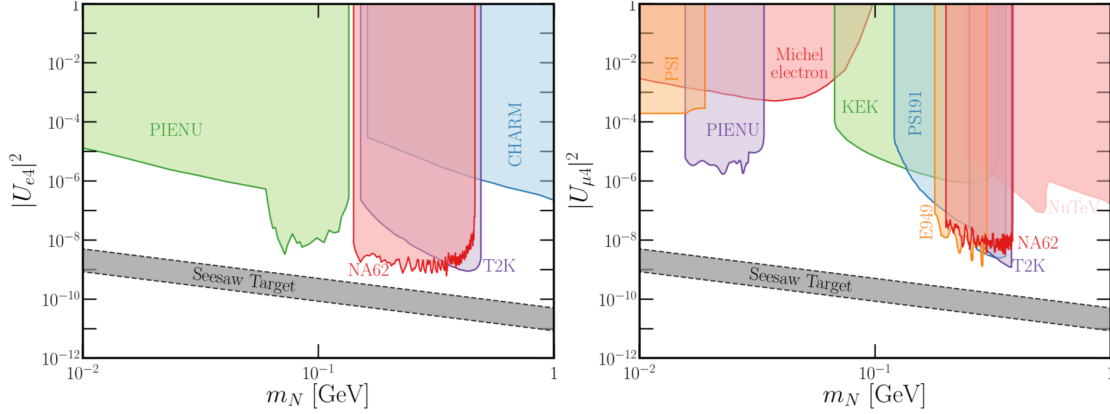


Figure 4: Experimental constraints on electron-coupled (left) and muon-coupled (right) HNLs as functions of their mass and the mixing $|U_{\ell 4}|^2$. NA62 results extend on a previously unexplored parameter space and complete the search for HNL in the $\pi \rightarrow \ell N$ channels. Figure from [17].

is also re-interpreted as a search for the decay $K^+ \rightarrow \mu^+ \nu X$, where X is a scalar or vector particle decaying to an invisible final state. Upper limits on the decay branching ratio for X masses in the range $10\text{--}370 \text{ MeV}/c^2$ are set ranging from $O(10^{-5})$ to $O(10^{-7})$ [14]. An improved upper limit of 1.0×10^{-6} is also established at 90% CL on the $K^+ \rightarrow \mu^+ \nu \nu \nu$ branching ratio [14].

4. Dark photon search in beam-dump mode

This section reports the preliminary results on a search for dark photon in-flight decay to $\mu^+\mu^-$ pairs, based on data collected by NA62 in 2021 when operating in beam-dump configuration. The data set corresponds to 1.4×10^{17} protons on target (POT) collected in 10 days of data taking with a rate of approximately 66×10^{11} protons per spill of 4.8 s effective duration. This intensity is equivalent to more than 1.5 times that for the nominal NA62 standard-beam operation.

Dark photons (DP) are predicted as one of the possible extension of the SM [18, 19] aiming to explain the abundance of dark matter in our universe. A new $U(1)$ gauge-symmetry sector with a vector mediator, the dark photon A' , is introduced. In a simple realization of such scenario, the A' field interacts with the SM hypercharge through a kinetic-mixing Lagrangian. The free parameters of the model are the mass $m_{A'}$ of the dark photon and the kinetic coupling constant $\varepsilon \ll 1$. In proton-nucleus interaction, dark photons can be produced via two different mechanisms: i) a bremsstrahlung-like production, and ii) a meson-mediated production. The two mechanisms differ in terms of production cross section and of momentum-angle spectra of the dark photon emitted. At the energy of the SPS protons, and given the feeble interaction of dark photon with SM particles, dark photons can travel tens of meters before decay reaching the NA62 decay volume. For masses $m_{A'}$ below $700 \text{ MeV}/c^2$, the dark photon decay width is dominated by decays to di-lepton final states. In the presented analysis, the di-muon final state is investigated.

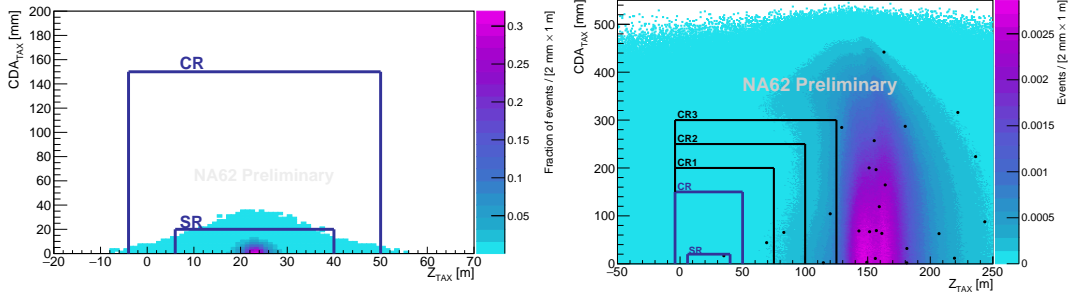


Figure 5: Closest distance of approach between the beam direction at the TAX entrance and the total momentum of the two muons (CDA_{TAX}) with respect to the longitudinal position of the primary vertex (Z_{TAX}). **Left:** Distribution of selected events from simulation in the control and signal regions. **Right:** Expected combinatorial background (color-scaled plot) and events from data (fill black dots). Data in the CR and SR are unblinded. Further regions surrounding the CR are also shown by the black lines.

The signal signature is defined by two opposite charged tracks forming a vertex within the detector fiducial volume. The point of closest distance of approach (CDA) between the reconstructed total momentum of the di-muon pair and the nominal proton beam line is then identified as the A' production position (primary vertex). The primary vertex is expected to lie near the beam impact point on the TAX. Signal and control regions are defined in the two-dimensional plane of CDA *versus* longitudinal coordinate of the primary vertex, Figure 5 left panel, and are selected as $\pm 3\sigma$ in each axis of the expected signal distribution. Both signal and control region are kept blind in data until the analysis is finalized. After signal selection the dominant background contribution is due to a random pairing of two halo muons from interactions of uncorrelated protons. Data

control samples, independent of those used for the signal selection, are defined and the background expectation is cross checked between data and simulation in different control regions, see right panel of Figure 5. Zero events are expected to be observed in both CR and SR with a probability of a non-zero observation in the SR of approximately 1.6%. After unblinding, no events are observed in the CR and one event, with approximately 411 MeV/ c^2 two-track invariant mass, in the SR. The corresponding observed 90% CL upper limit in the parameter space of the dark photon coupling and mass is shown as the region enclosed by black contour in the left panel of Figure 6. The excluded region improves on previous experimental limits in the mass range 200-500 MeV/ c^2 for mixing parameters of $O(10^{-6})$. As a counting experiment, the global significance of the observed event

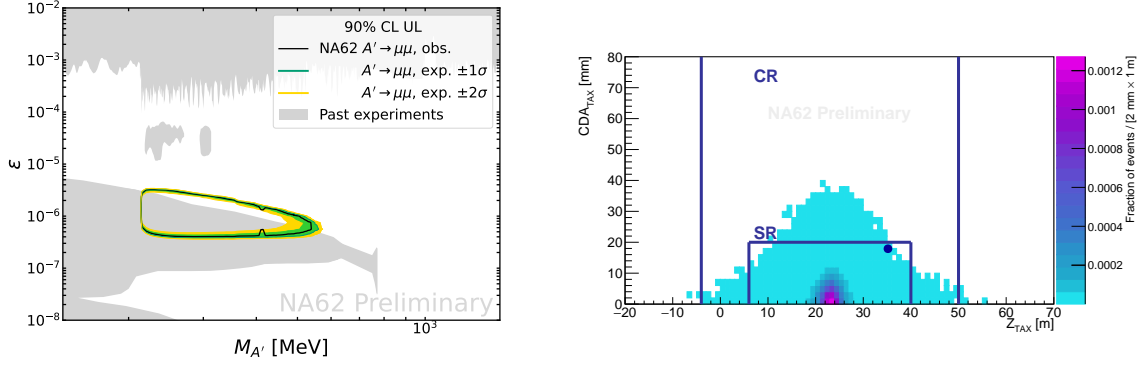


Figure 6: Left: The region of the parameter space within the solid black line is excluded at 90% CL. The green (yellow) filled area represents the expected uncertainty on the exclusion contour in absence of signal with 68% (95%) statistical coverage. **Right:** Distance of closest approach between beam direction at the TAX entrance and total momentum of the two tracks (CDA_{TAX}) vs the longitudinal position of the minimum approach (Z_{TAX}). Data (dots) and expected fraction of simulated signal events (color density) after opening both CR and SR.

is 2.4σ . However, the two-track time difference and their extrapolation to the TAX impact point (Figure 6 right panel) suggest that the observed event might be due to combinatorial background.¹ The quality of the NA62 data taken in beam-dump mode is adequate for other searches of dark sector particles. Among others, analysis are ongoing to search for dark-photon decays into e^+e^- final states, gluon-coupled axion-like particles decays to hadronic and $\gamma\gamma$ final states. To complete the search for new physics with beam-dump data, a total of about 10^{18} POT is expected to be collected during the whole NA62 Run2 (2021-2025) data-taking period.

5. Conclusions

NA62 is a multi-purpose experiment that, together with the main goal of $K^+ \rightarrow \pi^+\nu\bar{\nu}$ and precision measurements, covers a wide program of direct searches for new-physics phenomena, operating the experiment both in kaon and beam-dump configuration. Exploiting the data collected during the Run1 data-taking period, results have been presented for lepton number and lepton flavor violating processes in K^+ decays, as well as heavy neutral lepton production in $K^+ \rightarrow \ell^+N$ decays.

¹Note that, the shape of the expected signal within the SR is not used to determine the statistical significance.

First preliminary results using 2021 beam-dump data have been also presented for the search of dark photon decay to $\mu^+\mu^-$ final state.

References

- [1] E. Cortina Gil *et al* [NA62 Collaboration], *JHEP* **06** (2021) 093
- [2] E. Cortina Gil *et al* [NA62 Collaboration], *JINST* **12** (2017) P05025
- [3] R. Ammendola *et al*, *Nucl. Instrum. Meth. A* **929** (2019) 1
- [4] The NA62 Collaboration, *submitted to JHEP*, [[hep-ex:2208.00897](#)]
- [5] A. Atre *et al*, *JHEP* **05** (2009) 030
- [6] R. Mandal and A. Pich, *JHEP* **12** (2019) 089
- [7] A. M. Diamant-Berger *et al*, *Phys. Lett. B* **62** (1976) 485
- [8] R. L. Workman *et al* [Particle Data Group], *Prog. Theor. Exp. Phys.* **2022** (2022) 083C01
- [9] E. Cortina Gil *et al* [NA62 Collaboration], *Phys. Lett. B* **797** (2019) 134794
- [10] E. Cortina Gil *et al* [NA62 Collaboration], *Phys. Lett. B* **830** (2022) 137172
- [11] R. Aliberti *et al* [NA62 Collaboration], *Phys. Rev. Lett.* **127** (2021) 131802
- [12] E. Cortina Gil *et al* [NA62 Collaboration], *Phys. Lett. B* **838** (2023) 137679
- [13] E. Cortina Gil *et al* [NA62 Collaboration], *Phys. Lett. B* **807** (2020) 135599
- [14] E. Cortina Gil *et al* [NA62 Collaboration], *Phys. Lett. B* **816** (2021) 136259
- [15] T. Asaka and M. Shaposhnikov, *Phys. Lett. B* **620** (2005) 17
- [16] R. E. Shrock, *Phys. Lett. B* (1980) 159; *Phys. Rev. D* **24** (1981) 1232
- [17] E. Goudzovski *et al*, [[hep-ph:2201.07805](#)]
- [18] L. B. Okun, *Sov. Phys. JETP* **56** (1982) 502
- [19] B. Holdom, *Phys. Lett. B* **166** (1986) 196